Available online at www.sciencedirect.com

ScienceDirect

Physics Procedia 61 (2015) 729 – 736

Physics Procedia

Neutrino flavor evolution in turbulent supernova matter

Tina Lund and James P. Kneller

Department of Physics, North Carolina State University, 2401 Stinson Drive, Raleigh, NC 27695

Abstract

In order to decode the neutrino burst signal from a Galactic core-collapse supernova and reveal the complicated inner workings of the explosion, we need a thorough understanding of the neutrino flavor evolution from the proto-neutron-star outwards. The flavor content of the signal evolves due to both neutrino collective effects and matter effects which can lead to a highly interesting interplay and distinctive spectral features. In this paper we investigate the supernova neutrino flavor evolution by including collective flavor effects, the evolution of the Mikheyev, Smirnov & Wolfenstein (MSW) matter conversions due to the shock wave passing through the star, and the impact of turbulence. The density profiles utilized in our calculations represent a 10.8 $M_{\odot}$ progenitor and comes from a 1D numerical simulation by Fischer *et al.* [1]. We find that small amplitude turbulence, up to 10% of the average potential, leads to a minimal modification of the signal, and the emerging neutrino spectra retain both collective and MSW features. However, when larger amounts of turbulence are added, 30% and 50%, the features of collective and shock wave effects in the high density resonance channel are almost completely obscured at late times. At the same time we find the other mixing channels – the low density resonance channel and the non-resonant channels – begin to develop turbulence signatures. Large amplitude turbulent motions in the outer layers of massive, iron core-collapse supernovae may obscure the most obvious fingerprints of collective and shock wave effects in the neutrino signal but cannot remove them completely, and additionally bring about new features in the signal. We illustrate how the progression of the shock wave is reflected in the changing survival probabilities over time, and we show preliminary results on how some of these collective and shock wave induced signatures appear in a detector signal.

Selection and peer review is the responsibility of the Conference lead organizers, Frank Avignone, University of South Carolina,
and Wick Haxton, University of California, Berkeley, and Lawrence Berkeley Laboratory

Keywords: neutrino flavor oscillations, core-collapse supernovae, turbulence
PACS: 97.60.Bw, 14.60.Pq

1. Introduction

The neutrino signal from the next galactic core-collapse supernova (ccSN) will bring an unparalleled opportunity to learn about the explosion mechanism and the neutrino parameters. The current paradigm for the explosion mechanism of a core-collapse supernova entails an initial shock wave which stalls at roughly 200 km. The subsequent revival of the shock's outward movement some hundreds of milliseconds later is believed to be caused by the combined effect of neutrino heating, and convective large-scale mass motions or the Standing Accretion Shock Instability (SASI) [2, 3, 4, 5, 6, 7, 8, 9, 10]. With recent advances explosions in fully self-consistent 3 dimensional hydrodynamical simulations seem to be imminent. During their explosion ccSN release copious amounts of neutrinos, who carry away about 99% of the released gravitational energy. The next galactic ccSN will therefore generate an unprecedented large signal in the neutrino detectors here at Earth. This signal will provide us with an unrivaled opportunity to peer inside the ccSN, and to test the current explosion paradigm. For us to correctly decode the neutrino burst signal, though, requires a thorough understanding of the neutrino flavor evolution as the neutrinos propagate from the proto-neutron-star surface, through the turbulent matter to finally arrive at Earth. The flavor content will change over

Selection and peer review is the responsibility of the Conference lead organizers, Frank Avignone, University of South Carolina, and Wick Haxton, University of California, Berkeley, and Lawrence Berkeley Laboratory
doi:10.1016/j.phpro.2014.12.090

time due to the evolution of the neutrinos' self-interactions in the inner parts, and the interaction with the background matter at certain resonant densities, the so-called Mikheyev-Smirnov-Wolfenstein (MSW) effect, in the outer parts of the supernova. If the outer part of the supernova has turbulent motions these can create additional effects causing further flavor changes. The self-interactions are highly non-linear, and depend strongly on the neutrino luminosities and energies. At the present, this leaves us with very limited analytical predictive power except in the broadest sense. Investigations of neutrino self-interactions must therefore primarily be done through numerical calculations.

In this paper we investigate how the combined effect of neutrino self-interactions, neutrino matter interactions and turbulence affect the neutrino flavor evolution during the explosion of a $10.8\,M_\odot$ stellar progenitor. We will briefly explain the setup of our calculations in Sec. 2, and then we present our results in Sec. 3. We show both the neutrino flavor evolution in the matter basis and a preliminary example of how the neutrino signal would appear in a scintillator detector, before we give our conclusions in Sec. 4.

2. Description of the calculations

An accurate interpretation of a neutrino signal here on Earth, requires knowledge of how the neutrino flavor changes inside the supernova as a function of time. One must calculate the probability that a neutrino created in a certain flavor state exits the supernova in a given mass state, since mass states are the vacuum propagation eigenstates. To predict the neutrino flavor evolution we numerically solve a Schroedinger-like equation:

$$i\frac{\mathrm{d}S}{\mathrm{d}r} = (H_{vac} + H_{mat} + H_{\nu\nu})\; S \tag{1}$$

Here, the S-matrix evolves the neutrino wave function from time t_0 to t, $\Psi(t) = S(t_0, t)\,\Psi(t_0)$, and gives the probability that a neutrino created in one state ν_j will be found later in state ν_i; $P_{\nu_j\rightarrow\nu_i} = |S_{ij}|^2$. For the antineutrino quantities we will use $\bar{P}$ and $\bar{S}$. The part of the Hamiltonian that describes the neutrino propagation in vacuum is diagonal in the mass basis, and proportional to the neutrino energy, E, and one of the two neutrino mass splittings, $H_{vac} \propto \Delta m^2_{ij}/2E$. The unitary Pontecorvo-Maki-Nakagawa-Sakata (PMNS) mixing matrix that relates the mass basis to the flavor basis, $\nu_\alpha = U_{PMNS}\,\nu_i$, can be parameterized by three mixing angles, θ_{12}, θ_{13} and θ_{23}, a CP-violating phase, δ, and two Majorana phases α_1 and α_2. The latter two phases will not influence the neutrino flavor mixing and we will ignore them henceforth. For our calculations we use the most up to date values of the vacuum mixing angles, $\theta_{12} = 34.4°$, $\theta_{13} = 9°$, $\theta_{23} = 45°$, and we set $\delta = 0$. For the neutrino mass splittings we use: $\Delta m^2_{21} = 7.59 \times 10^{-5}$ eV^2 and $\Delta m^2_{32} = 2.43 \times 10^{-3}$ eV^2, and we consider both the normal hierarchy (NH) and the inverted hierarchy (IH). For doing the actual calculations the matter basis is the most practical one, since it closely aligns with the flavor states at the neutrinosphere and with the mass states in vacuum. The mixing matrix relating the vacuum mass states to the matter states has the same structure as the PNMS matrix, but now the mixing angles depend on the instantaneous density. The neutrino self-interaction part of the Hamiltonian in Eq. 1 contains highly non-linear terms relating the behavior of one neutrino to the evolution of all other neutrinos and anti-neutrinos. In the flavor basis $H_{\nu\nu}$ can be written as

$$H_{\nu\nu} \propto \frac{\sqrt{2}\,G_F}{2\,\pi\,R_\nu^2}\left\{\int dE_\nu\, S(r, E_\nu)\,\rho(r_0, E_\nu)\,S^\dagger(r, E_\nu) - \int dE_{\bar{\nu}}\left(\bar{S}(r, E_{\bar{\nu}})\,\bar{\rho}(r_0, E_{\bar{\nu}})\,\bar{S}^\dagger(r, E_{\bar{\nu}})\right)^\star\right\} \quad , \tag{2}$$

where G_F is the Fermi constant and R_ν is the radius of the neutrino sphere, which we take to be 10 km. The neutrino density matrix $\rho(r_0, E_\nu)$, and similarly anti-neutrino density matrix $\bar{\rho}(r_0, E_{\bar{\nu}})$, depends on the neutrino energies and the initial point, r_0, which we take to be 70 km. In order to make the calculations tractable, we have chosen to work in the single angle approximation. Though the validity of the single angle approximation remains under debate, it was shown by Sarikas *et al* [11] that the results of single angle calculations can match those from full multi-angle calculations. The matter part of the Hamiltonian is diagonal in flavor space, and proportional to the instantaneous electron density, $H_{mat} \propto \sqrt{2}\,G_F\,n_e(r)$. For antineutrinos the matter effect is opposite, leading to a minus sign in the equation. The information on the matter density, $\rho(r)$, and electron fraction, Y_e, for our calculations comes from 1D simulations by Fischer *et al.* [1]. From these simulations we also use the information on neutrino luminosities, L_ν, and energies, E_{mean} and E_{rms}. The time evolution of these quantities is shown in Fig. 2. We use a "pinched" spectrum as described in Keil *et al.* [12] to model the neutrino spectra. The $10.8\,M_\odot$ progenitor, that is our focus in this paper[1], was

[1] Investigations of a lighter and a heavier progenitor as well as further details can be found in [13].

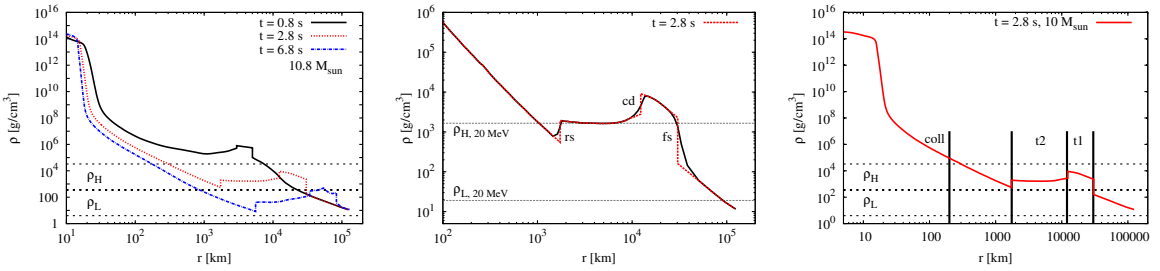

Figure 1: Density profiles at $t = 0.8$, 2.8 and 6.8 s (left), and $t = 2.8$ s (middle and right). Horizontal dashed lines mark the high density, H, and low density, L, resonant regions. Vertical lines in the right most panel indicate the regions where collective effects dominate (coll) and where turbulence has been added (t1, t2). The black curve in the middle panel is the original profile, the red curve is the steepened version. The positions of the forward shock (fs), reverse shock (rs) and the contact discontinuity (cd) have also been marked.

simulated until 10.7 s after bounce. We have followed the time evolution by investigating the neutrino evolution along multiple density profiles at 1s intervals in the cooling phase of the supernova ($t \gtrsim 0.5$ s). A few representative density profiles can be seen in the left panel of Fig. 1, where the development of the reverse shock (rs) and the movement of the forward shock (fs) over time can be seen. The bands marked ρ_H and ρ_L show the resonant densities for neutrinos with energies in the range 1–100 MeV for the high density (H) resonance and the low density (L) resonance respectively. The H resonance corresponds to the mass splitting Δm_{32} and the L resonance corresponds to the Δm_{21} mass splitting. The middle panel show a close up of the 2.8 s profile, and the contact discontinuity (cd), reverse and forward shocks have been indicated. We had to steepen the initial profiles by hand due to the coarse resolution of the simulations. The steepened version of the density profile is shown in red, and the original profile is in black in the middle panel of Fig. 1. The horizontal gray dashed lines show the resonant densities for a 20 MeV (anti-)neutrino.

Adding turbulence to the inherently non-turbulent 1D potential is done by multiplying a Gaussian random field $F(r)$ onto the average potential, $\langle V_e \rangle$. Our implementation follows the prescription given in Kneller & Volpe [14], where: $V_e(r) = (1 + F(r))\,\langle V_{e,0} \rangle$, with

$$F(r) = C_* \tanh\left(\frac{r - r_{rs}}{\lambda}\right) \tanh\left(\frac{r_{fs} - r}{\lambda}\right) \times \sum_{n=1}^{N_k} \sqrt{V_n}\ (A_n \cos(k_n r) + B_n \sin(k_n r))$$

We have used a Kolmogorov power spectrum, and investigated turbulence amplitudes of $C_* = 0.1, 0.3$ and 0.5. The inclusion of the two hyperbolic tangents is to ensure the turbulent area subsides naturally into the non-turbulent areas, and the damping scale λ is taken to be 100 km. The expectation value of $F(r)$ is by construction made to vanish, and the method used to construct the variables k_n, A_n, B_n and V_n is based on the Randomization method 'Variant C' from

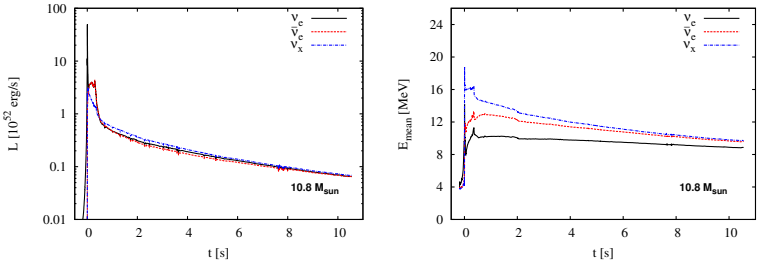

Figure 2: Neutrino luminosities, L (left), and mean energies, E_{mean} (right), for the 10.8 $M_\odot$ progenitor covering the 10.7 s time duration of the simulation. The quantities for $\bar{\nu}_x$ are similar to those of its partner ν_x and are therefore not shown here.

Kramer, Kurbanmuradov & Sabelfeld [15]. We include two regions of turbulence; one between the forward shock, r_{fs}, and the contact discontinuity, r_{cd}, and a second region between the contact discontinuity and the reverse shock, r_{rs}, once that has formed. In the right panel of Fig 1 we show on the 2.8 s profile where the turbulence is inserted.

3. Results

We have found it instructional to divide the density profiles into an "inner region", below 1000 km, where the collective effects are expected to dominate the flavor evolution, and an "outer region", where MSW effects and turbulence are dominating the flavor conversions. We then performed four calculations on each density profile: One that covers only the inner region, one that covers the outer region, and two calculations covering the full density profile, one without and the other with turbulence added to the potential. Below we will step through the results of the calculations performed on the density profile at 2.8 s post bounce (pb), and explain which features are caused by which interaction. We have chosen the density profile at 2.8 s, since at this time the star has developed both a contact discontinuity, a forward and a reverse shock. Furthermore, at this time the forward shock is far enough out in the star to affect the H resonance. The results of our calculations in the neutrino matter basis are given in Fig. 3. An explanation of how to read this figure is in order. Fig. 3a and Fig. 3b consists of 6 quartets each. Within each quartet the top panels show the survival probability of each neutrino (right) and antineutrino (left) matter state, and the bottom panels show one

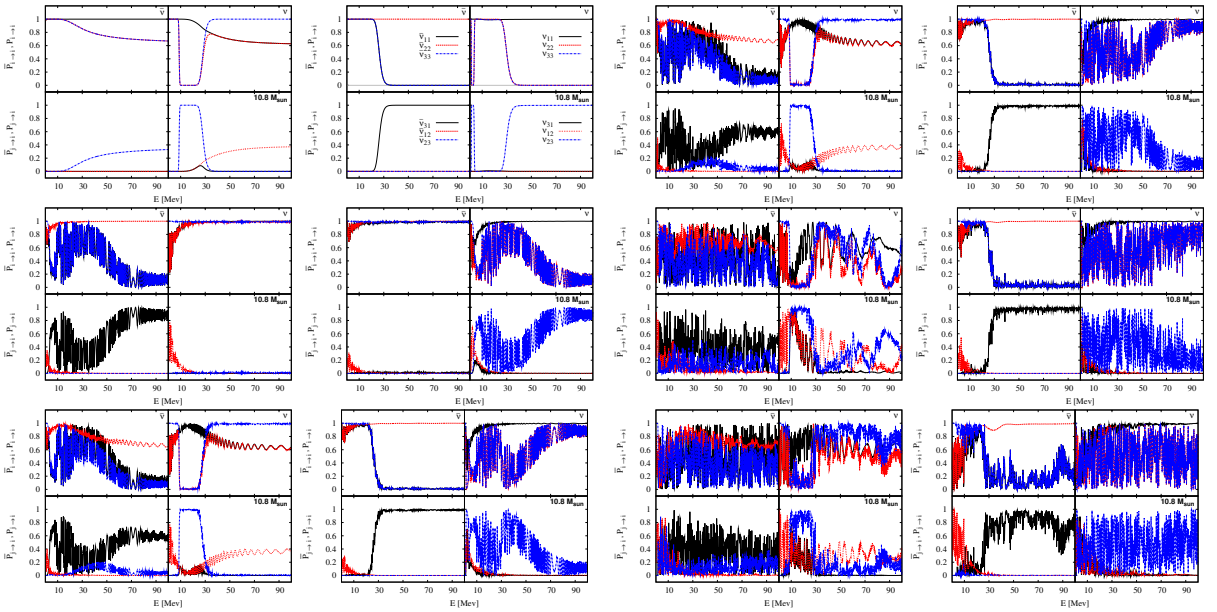

(a) (b)

Figure 3: Matter state survival and transition probabilities for $\bar{\nu}$ (*left* panels of each quartet, $\bar{P}$) and ν (*right* panels of each quartet, P) for calculations on the density profile at 2.8 s pb from the 10.8 $M_\odot$ progenitor. Survival probabilities, $P_{\nu_i\to\nu_i}$ and $\bar{P}_{\nu_i\to\nu_i}$, are shown in the upper panels of each quartet, and transition probabilities, $P_{\nu_j\to\nu_i}$ and $\bar{P}_{\nu_j\to\nu_i}$, are shown in the bottom ones. The solid black lines indicate the probabilities for ending in matter state 1 (or anti-matter state $\bar{1}$ in the case of anti-neutrinos), the red dashed lines give the probabilities of ending in matter state 2 ($\bar{2}$) and finally the blue dot-dashed lines give the probabilities for ending in matter state 3 ($\bar{3}$) at the end of the calculation domain. Fig. 3a show the calculations without turbulence: a calculation for the inner region at the top, a calculation of only the outer region in the middle and a calculation for the full density profile at the bottom. In Fig. 3b all calculations cover the full density profile but with turbulence added; 10% in the top quartets, 30% in the middle and 50% in the bottom quartets. In each subfigure the left quartets are for calculations done in the inverted hierarchy, and the right quartets are for calculations done in the normal hierarchy.

transition probability for each neutrino (right) and antineutrino (left) matter state, as a function of the (anti-)neutrino energy. The last transition probability can be inferred from the transition probability and survival probability given here since the sum of all three probabilities is one.

3.1. Collective effects, matter effects and their combination

The matter probabilities after the neutrinos have propagated to 1000 km are shown in the top two quartets of Fig. 3a. In this region we expect the neutrino self-interaction to dominate the flavor evolution. We see that abrupt drops in survival probability appear for both neutrinos and antineutrinos. In the IH (left column) the flavor conversion for antineutrino states $\bar{2}$ and $\bar{3}$ is only partial, the survival probability drops from $P = 1$ to $P \simeq 0.67$, but it happens for all antineutrinos with energies above 20 MeV. For the neutrinos there is a full conversion of states 2 and 3 for neutrinos with energies between 8 MeV and 28 MeV, where the survival probability drops from $P = 1$ to $P = 0$. From the lower panel we see that at the energies where the survival probabilities go to zero, the transition probability for neutrino state 2 going to state 3 goes to one. Combined with the fact that neutrino state 3 does not substantially convert into state 1 (black line, lower right panel of the quartet), this indicates an almost full conversion between neutrino matter states 2 and 3. Between neutrino states 1 and 2 a partial conversion takes place for neutrinos with energies higher than ∼20 MeV. In the NH (right column) we see that a full conversion now takes place in the antineutrino channel, this time between antineutrino states $\bar{1}$ and $\bar{3}$ with energies above 27 MeV. The neutrino channel exhibits 3 spectral splits; at 2 MeV, 4 MeV, and 30 MeV, causing full conversions between neutrinos states 2 and 3 in the energy region between the two lowest energies and for all neutrinos with energies above 30 MeV.

Moving to the outer region where the MSW effect is dominant, we focus on the middle two quartets. The neutrino and antineutrino matter probabilities in both hierarchies show an interesting feature; a drop in the survival probabilities of states 1 and 2 ($\bar{1}$ and $\bar{2}$) at 1-2 MeV. The drops are deeper for the neutrino states (in either hierarchy) and these are caused by the forward shock having reached the densities where low energy neutrinos have their L resonance (see the right most panel of Fig. 1 for the band of resonant densities and the position of the forward shock). The forward shock is partially in the H resonant density regions, and the effect of that shows itself for neutrinos in the NH (right column) and for the antineutrinos in the IH (left column). The features that are induced are very similar. For the antineutrinos the H resonance leads to a conversion of matter states $\bar{1}$ and $\bar{3}$ in the IH, and for the neutrinos, the H resonance leads to a conversion of matter states 2 and 3 in the NH. The first thing to note is the overall undulating trend of the survival probability: There is an initial drop at 4 MeV, followed by a return to almost unit survival probability above 12 MeV with finally a drop to zero survival probability for energies above ∼50 MeV. The matter induced spectral splits seen at 4 MeV and 12 MeV for both neutrinos and antineutrinos are caused by the contact discontinuity providing one diabatic resonant conversion for neutrinos with energies in this range. Similarly the swap at energies higher than roughly 50 MeV is caused by the single diabatic resonant conversion provided by the forward shock. The left panel of Fig. 4 illustrate the single and multiple resonances encountered by neutrinos with different energies. On top of the general undulating trend in Fig. 3a one sees rapid fluctuations. These are caused by phase effects because each neutrino encounters multiple sequential adiabatic and diabatic resonances as it propagates out [16, 17]. An example of the multiple resonances encountered, can be seen in the middle panel of Fig. 1, where the gray dashed lines indicate the resonant densities for a 20 MeV (anti)neutrino.

The bottom two quartets in Fig. 3a show the results of a calculation covering the full profile. We see that, for the most part, the final features here are a straight forward superposition of the features induced by the collective effect and the MSW effect separately. For instance the collective split at ∼30 MeV for antineutrino in the NH is easily recognized in the results of the full calculation. Similarly, the overall undulating trend in the antineutrino survival probability in the IH caused by the matter effect is easily visible in the full calculation. However, in the neutrino survival probabilities in the NH a new feature seems to have arisen. At 30 MeV there now appears a split, causing the survival probabilities at higher energies to be inverted compared to the appearance for the outer region alone. This is because for neutrinos with energies above 30 MeV the matter states 2 and 3 have already been converted by the collective effect. This initial conversion between the two states is subsequently reversed partially by the matter effect. Thus, the superposition of features from the inner and outer regions in the full calculation is easily understood. One effect takes place after the other, occasionally causing conversion between two previously interchanged neutrino states.

3.2. Turbulence

With an understanding of the features induced by the collective and matter effects separately and in combination, we can turn to the calculations that include turbulence. In Fig. 3b we show the probabilities resulting from calculations with 10% (top two quartets), 30% (middle two quartets) and 50% (bottom two quartets) turbulence added to the potential of the $10.8\,M_\odot$ at 2.8 s pb. Comparing the top most quartets with the bottom most ones of Fig. 3a we see only very minor changes. The rapid oscillations caused by the phase effect seem to be amplified. This blurs the spectral splits in the resonant channels, but the overall undulating trend in both neutrinos and antineutrinos, however, remain clearly visible. Increasing the amount of turbulence to 30% brings drastic changes in the survival probabilities. The enhancement of the phase effects obscures the general trend in the antineutrinos in the IH, and for the neutrinos only a weak remnant of the trend is left at high energies in the NH. The spectral splits induced by the self-interactions, at 30 MeV for the antineutrinos in the NH, and at 8 MeV and 28 MeV in the neutrino probabilities in the IH, fortunately remain visible, but additional fluctuations have appeared in the survival probabilities, most notably in the neutrino states. Although the addition of 50% turbulence at a first glance looks even more discouraging, there is a silver lining: The two distinct spectral splits in the IH for neutrinos, and the single spectral split in the antineutrinos in the NH, caused by collective effects, remain visible. Furthermore, although 50% turbulence obscures completely the overall trends in the high density resonant channels; the features in the neutrino survival probabilities in the NH and the antineutrino features in the IH, then it brings about new features in the non-resonant channels. Looking closely at the survival probability of the antineutrino states $\bar{1}$ and $\bar{3}$ in the NH, the average survival probability of the antineutrino states with energies above 30 MeV is now ∼0.2 instead of the 0 it was when there was no or less than 50% turbulence. This means we would get an admixture of the higher energy non-electron neutrino spectrum into the final electron flavor spectrum, making it easier to observe with current detector technology.

By comparing all the figures with turbulence we note the important fact that the collectively induced splits at 8 and 28 MeV in the IH for neutrino states 2 and 3 remain visible through all amounts of turbulence. As does the spectral split at 27 MeV in the antineutrino states $\bar{1}$ and $\bar{3}$ in the NH. Surviving the turbulence shows that the collective features are robust, and if these collective features make their way through to the observed signal then we can make definite statements about the neutrino hierarchy.

3.3. Time evolution of features

The above discussion of features in the neutrino matter state probabilities focused on a single snapshot in time. However, as time passes features induced by self-interactions and from matter interactions wax and wane. One feature of particular interest is caused by the forward shock. The outward movement of the shock, and thus its progression into lower densities, can be followed in the changes of the neutrino matter state survival probabilities. In the left panel of Fig. 4 we show 4 density profiles from 1.8 s pb and to 6.8 s pb. The gray and black horizontal lines show the resonant density for the H and the L resonance respectively for a neutrino with the energy indicated. The "outer region" survival probabilities for neutrino matter state 3, P_{33}, in the NH, corresponding to the density profiles, plus two additional ones, are shown in the right panel of Fig. 4. The diabaticity of the forward shock causes a full flavor conversion in the relevant density regions for neutrinos of appropriate energies, thus the survival probability drops from $P = 1$ to $P = 0$. In the right panel of Fig. 4 we have marked the drop feature in question with a black arrow on the P_{33} survival probability at 4.8 s pb (blue dot-dashed line). The fact that the drop spans several energies is due to the finite width of the resonance. As the density range covered by the shock front moves into lower densities, bringing higher energy neutrinos into resonance, and making lower energy neutrinos non-resonant, the drop feature in the survival probability moves to progressively higher energies. We see how the midpoint of the drop moves from about 4 MeV at 2.8 s, to 25 MeV at 4.8 s, to 56 MeV at 5.8 s. At 6.8 s the drop is beginning to slip out of the energy range we consider and by 7.8 s it has vanished. Were it possible to observe this drop in survival probability caused by the contact discontinuity and the forward shock, and follow its progression in energy over time, it should be possible to map that back to the movement of the forward shock.

3.4. Signatures in observable neutrino signals

The clear features from self-interactions and matter interactions seen in the matter survival probabilities give hope that we might actually observe some of these features. To test how well we might identify these features in an observed neutrino signal, we use the software SNOwGLoBES [18] to generate a signal in a 50 kt scintillator detector based on

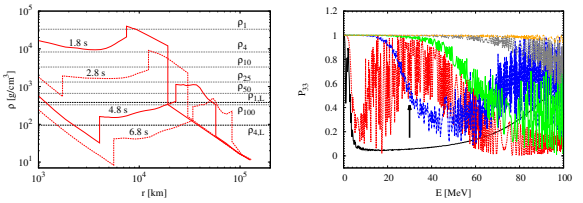

Figure 4: Left: Density profiles for various times (red lines). Horizontal dashed lines indicate the resonant densities corresponding to a neutrino with the given energy for the H resonance (gray) and the L resonance (black). Right: Survival probability for ν matter state 3, P_{33}, corresponding to times 1.8 s (black), 2.8 s (red), 4.8 s (blue), 5.8 s (green), 6.8 s (gray) and 7.8 s (yellow).

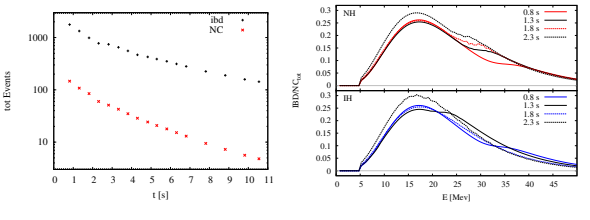

Figure 5: Left: Number of inverse beta decay (ibd) and neutral current (NC) events expected in a 50 kt scintillator detector if the supernova was at 10 kpc. Right: inverse beta decay events scaled by the total number of NC events at that time.

the neutrino fluxes that resulted from our calculations. We show a few preliminary results in Fig. 5. In the left panel we show the total number of neutral current (NC) events and inverse beta decay (IBD) events as a function of time, assuming a distance to the supernova of 10 kpc. The "kink" seen in both graphs, at roughly ~ 2.5 s, is caused by a reduction in the neutrino luminosity when the reverse shock is formed. We note that the slope of the NC event curve is slightly steeper than the one for the IBD events. In the right panel of Fig. 5 we show the number of IBD events, divided by the total number of NC events (at that time), as a function of energy for assumptions of a normal hierarchy (upper part) or an inverted hierarchy (lower part). The first thing to note is that over this brief time window there is a significant difference in the evolution of the signal appearance in the two hierarchies, enabling us to distinguish the two hierarchies in an actual observation. In the NH results, we see a plateau like feature around 35 MeV at 0.8 s. In the subsequent time snapshots this feature moves to lower energies. This plateau like feature corresponds to the self-interaction feature that can be seen at 27 MeV at 2.8 s in the upper right quartet of Fig. 3a for the antineutrino states $\bar{1}$ and $\bar{3}$. The collective effects change over time, causing the exact energy where the conversion happens to move around (see also our full paper [13] for more information). Turning our attention to the IH (lower panel) at 0.8 s, we see a similar plateau, however this time it appears to move to lower energies much more rapidly and disappear within the next second. This interpretation is only partially correct. The plateau observed at 0.8 s is caused by the neutrino self-interaction, as in the NH, but the plateau seen at 1.3 s at roughly 22 MeV, is actually due to the shock wave making the H resonance diabatic in the antineutrino channel.

Summarizing this brief preliminary investigation of the signal appearance we find that: Features of the collective effects appear to be visible in a predicted signal, and remain visible for some time. The impact of the shock wave in the resonant channel on the other hand is very brief. The differences in the results for the two hierarchies are marked enough that when one includes the time evolution it should be possible to distinguish them.

4. Conclusions

This paper has investigated the influence of neutrino self-interactions, matter interactions and turbulence on the flavor evolution of ccSN neutrinos. We have focused the investigation on a 10.8 $M_\odot$ progenitor that was simulated in 1D for 10.7 s pb. We have considered the effect of collective and MSW effects both separately and in combination. Both effects leave their own distinct signatures in the neutrino matter survival probabilities. For calculations covering the full profiles, we find that the flavor conversion induced by the two effects is in some sense additive. This holds even with the time variation seen in the impact of both the collective and matter effect. The addition of modest amounts of turbulence does not significantly obscure the features engendered by collective and matter effects. Large amounts, on the other hand, obscure some of the most prominent features. At the same time though, the large turbulence generates mixing in the non-resonant neutrino channels. By tracking the evolution of the neutrino survival probabilities over time, we find that they can give information about the shock propagation within the star. A preliminary investigation shows that both collective and shock wave features are potentially observable in a neutrino signal captured with a scintillator detector, but a more detailed study is needed to make firm predictions.

References

[1] T. Fischer, S. C. Whitehouse, A. Mezzacappa, F.-K. Thielemann, M. Liebendörfer, Protoneutron star evolution and the neutrino driven wind in general relativistic neutrino radiation hydrodynamics simulations, A&A 517A (2010) 80F.
[2] J. W. Murphy, C. Meakin, Astrophysics Journal 74 (2011) 742.
[3] C. D. Ott, E. Abdikamalov, P. Moesta, R. Haas, S. Drasco, et al., Astrophysics Journal 768 (2013) 115.
[4] J. C. Dolence, A. Burrows, J. W. Murphy, J. Nordhaus, Astrophysics Journal 765 (2013) 110.
[5] F. Hanke, A. Marek, B. Müller, H.-T. Janka, Astrophysics Journal 755 (2012) 138.
[6] O. Pejcha, T. A. Thompson, Astrophysics Journal 746 (2012) 106.
[7] B. Müller, H.-T. Janka, A. Heger, Astrophysics Journal 761 (2012) 72.
[8] T. Takiwaki, K. Kotake, Y. Suwa, Astrophysics Journal 749 (2012) 98.
[9] E. J. Lentz, S. W. Bruenn, J. A. Harris, M. A. Chertkow, W. R. Hix, et al., PoS NICXII (2012) 208.
[10] Y. Suwa, K. Kotake, T. Takiwaki, S. C. Whitehouse, M. Liebendoerfer, K. Sato, Publ. Astron. Soc. Jap. 62 (2010) L49.
[11] S. Sarikas, D. de Sousa Seixas, G. Raffelt, Phys. Rev. D 86 (2012) 125020.
[12] M. T. Keil, G. G. Raffelt, H.-T. Janka, Monte Carlo Study of Supernova Neutrino Spectra Formation, The Astrophysical Journal 590 (2003) 971–991, [arXiv: astro-ph/0208035v2].
[13] T. Lund, J. P. Kneller, Combining collective, MSW, and turbulence effects in supernova neutrino flavor evolution, Phys. Rev. D 88 (2013) 023008.
[14] J. P. Kneller, C. Volpe, Turbulence effects on supernova neutrinos, Phys. Rev. D 82 (2010) 123004.
[15] P. R. Kramer, O. Kurbanmuradov, K. Sabelfeld, Journal of Computational Physics 226 (2007) 897.
[16] J. P. Kneller, G. C. McLaughlin, Monte carlo neutrino oscillations, Phys. Rev. D 73 (2006) 056003.
[17] B. Dasgupta, A. Dighe, Phase effects in neutrino conversions during a supernova shock wave.
[18] B. et al, SNOwGLoBES: SuperNova Observatories with GLoBES: Draft, unpublised.